

8/24/93  
E8013

NASA Technical Memorandum 106276

# Protective Coatings for High-Temperature Polymer Matrix Composites

David R. Harding  
*Sverdrup Technology, Inc.*  
*Lewis Research Center Group*  
*Brook Park, Ohio*

James K. Sutter  
*National Aeronautics and Space Administration*  
*Lewis Research Center*  
*Cleveland, Ohio*

and

Demetrios S. Papadopoulos  
*Case Western Reserve University*  
*Cleveland, Ohio*

Prepared for the  
25th International SAMPE Technical Conference  
sponsored by the Society for the Advancement of Material and  
Process Engineering  
Philadelphia, Pennsylvania, October 26–28, 1993

The NASA logo, consisting of the word "NASA" in a bold, sans-serif font.

# PROTECTIVE COATINGS FOR HIGH-TEMPERATURE POLYMER MATRIX COMPOSITES

David R. Harding  
Sverdrup Technology, Inc.  
Lewis Research Center Group  
Brook Park, Ohio 44142

James K. Sutter  
National Aeronautics and Space Administration  
Lewis Research Center  
Cleveland, Ohio 44135

Demetrios S. Papadopoulos  
Case Western Reserve University  
Cleveland, Ohio 44106

## ABSTRACT

Plasma-enhanced chemical vapor deposition was used to deposit silicon nitride on graphite-fiber-reinforced polyimide composites to protect against oxidation at elevated temperatures. The adhesion and integrity of the coating were evaluated by isothermal aging (371 °C for 500 hr) and thermal cycling. The amorphous silicon nitride (a-SiN:H) coating could withstand stresses ranging from approximately 0.18 GPa (tensile) to -1.6 GPa (compressive) and provided a 30 to 80 percent reduction in oxidation-induced weight loss. The major factor influencing the effectiveness of a-SiN:H as a barrier coating against oxidation is the surface finish of the polymer composite.

**KEY WORDS:** Coating, Polymer matrix composite, Oxidation reduction

## 1. INTRODUCTION

Currently, a limiting factor in the application of polymer matrix composite (PMC) materials in aircraft frames and engines is the high-temperature performance of the resin.<sup>(1)</sup> The primary benefit in replacing metals with lower density, higher specific strength PMC's is the weight savings. Additional advantages are the lower processing and fabrication costs. A major limitation

to using PMC's at elevated temperatures is the oxidation of the polymer resin, which degrades the mechanical properties. Numerous synthetic approaches are underway to improve the long-term thermo-oxidative stability to a target temperature of 425 °C (800 °F) by eliminating the oxidative weak-point at the ends of the polymer chain<sup>(2)</sup> while retaining the desirable rheological properties of the resin.

A PMC system using the PMR-II-50 resin demonstrates the optimum blend of high mechanical strength, good processability (viscoelasticity), and high-temperature stability required for aerospace applications. This study investigates whether a protective coating can extend the useful lifetime or maximum use temperature of PMC's by retarding the oxidation of the resin. Implicitly, this coating must provide an adherent, dense, oxidation-resistant diffusion barrier that limits oxygen penetration to the resin's surface.

A major concern with coated materials in high-temperature applications is the thermal stress created by the mismatch in the coefficients of thermal expansion  $\alpha$  of the PMC substrate and the coating. The overall  $\alpha$  for a PMC is determined by the fiber volume and orientation of a low- $\alpha$ , high-stiffness carbon fiber in a high- $\alpha$ , low-stiffness resin matrix. A large thermal stress gradient component is to be expected because of the required temperature range ( $\Delta T = 400$  °C). Consequently, a coating material would have to be ductile or possess a high yield strength.

The suitability of the available coating techniques is governed by the temperature threshold of the polymer resin, the roughness of the PMC surface, and the necessity of coating geometrically complex shapes. Initially, three coating procedures were considered: (1) a sol-gel solution dip process, (2) physical vapor deposition (PVD), and (3) chemical vapor deposition (CVD). The solution dip process is ideally suited to coating complex shapes, but the high temperatures (in excess of the vaporization temperature of the polymer resin) required to solidify the organic precursors into a dense, pore-free oxidation barrier<sup>(3)</sup> would irreparably damage the mechanical properties of the PMC. This temperature constraint focused further research toward PVD and CVD. PVD can readily deposit coatings (especially metals) on substrates at comparatively low temperatures (within the threshold of the PMC) and is a straightforward procedure with an extensive literature base; however, it is primarily a line-of-sight technique, which complicates the coating of PMC components that have complex shapes. In a previous study<sup>(4)</sup> a superalloy, nickel chromium aluminum yttrium (NiCrAlY), was sputter deposited on PMR-15 PMC's. NiCrAlY was selected because of its large  $\alpha$ , which should reduce the potential thermal stress.

This paper discusses a specialized version of the thermal CVD technique—plasma-enhanced CVD—to deposit amorphous silicon nitride (a-SiN:H) coatings. The technique uses the electron energy in a capacitively coupled plasma to dissociate precursor gases for subsequent deposition and chemical reaction on the surface. Consequently, a temperature can be selected that will yield an optimum combination of coating morphology, film stress, and growth rate without having to consider the temperature required to initiate thin film growth. These a-SiN:H coatings are widely used in the microelectronics industry as passivating and protective coatings. They are dense and hard, serve as an effective diffusion barrier, and can be deposited at temperatures below 300 °C.<sup>(5)</sup>

The stiffness and brittleness of amorphous, plasma-deposited silicon nitride is markedly different from sintered, hot-pressed, or CVD polycrystalline, pyrolytic silicon nitride.<sup>(6,7)</sup>

## 2. EXPERIMENTAL PROCEDURE

**2.1 Laminate Processing** The PMR-II-50 monomer solutions were prepared with p-phenylene diamine, 6F dianhydride, and 1,2-norbornene monomethyl ester carboxylic acid (NE). The dimethyl esters of 6F dianhydride (6FDE) were dissolved in anhydrous methanol to form a 50 wt % PMR-II monomer solution with a stoichiometric ratio of n mol of 6FDE, n + 1 mol of diamine, and 2n mol of NE. The formulated molecular weight of the imidized prepolymer was 5000 amu, with an n value of 9.

All laminates were prepared from unidirectional graphite-fiber- (Amoco T650-42) reinforced prepreg tape. PMR-II-50 monomer methanol solutions were applied to the drum-wound unidirectional fiber to yield ~58 vol % laminates. Then the prepreg was dried on the drum to a volatile content of 11 to 12 wt % and cut into 7.6- by 20.3-cm plies. Twelve-ply laminates were manufactured from the prepreg stack by compression molding<sup>(2)</sup> or simulated autoclave vacuum-bag molding.<sup>(8)</sup>

Pulse echo ultrasonic C-Scan analysis was performed at 0.125-cm increments on both sides of the 12-ply laminates with a Physical Acoustics Corporation 2.5-MHz transducer. Specimens for coating were cut from high-quality areas of each laminate (void content <4 vol %). Void volumes, which were measured according to ASTM D 2734-70 (reapproved 1985), ranged from 2 to 6 vol %. Fiber content was 64±2 vol %.

**2.2 Coating Deposition** The plasma-enhanced CVD apparatus consisted of a capacitively coupled parallel-plate electrode configuration with a powered (13.56-MHz) "shower-head" top electrode and a heated, grounded bottom electrode (20-cm diameter molybdenum) that served as the substrate holder. Silicon nitride (a-SiN:H) was deposited from silane, hydrogen, ammonia, nitrogen, and argon precursor gases (MG Industries): 5 percent SiH<sub>4</sub> (99.95 percent pure) in H<sub>2</sub> (99.999 percent pure), NH<sub>3</sub> (99.99 percent pure), N<sub>2</sub> (99.999 percent pure), and Ar (99.999 percent pure). Growth rates of 300 Å/min at 0.75 torr and flow rates of 500 sccm were achieved. The PMC coupons were coated on both sides under various conditions (Table 1) then cleaned in a 2-percent (series 8790) micro solution (Cole Pamer) for 5 min followed by a 2-min deionized water rinse and air drying.<sup>(9)</sup> Si(100) witness wafers (cleaned in ethanol and 10-percent HF solutions) were included in all experiments to provide a reproducible substrate for composition analysis and measuring stresses.

**2.3 Coating Composition and Evaluation** Techniques used included x-ray photoelectron spectroscopy (VG ESCALAB Mk II, Vacuum Generators) for surface elemental identification, analytical electron microscopy (wavelength dispersive spectroscopy) (JEOL 840, Japanese Electro-Optic Laboratories) to quantify the coating composition, Fourier transform infrared spectroscopy (Nicolet) to identify infrared-active bonds present in the coating, Rutherford backscattering (SUNY Albany Dynatron) to quantify and depth profile the coating composition,

and a nuclear resonance technique<sup>(10,11)</sup> to measure the hydrogen content of the silicon nitride coatings.

The adherence and resilience of the coating, as-deposited and when thermally aged, was observed with a JEOL 840 electron microscope. At different stages of the testing cycle, samples were metallurgically cross-sectioned to establish the uniformity of the coating and to identify deteriorations in the coating once the PMC is aged.

Internal stresses in the a-SiN:H coatings were calculated from the radius of curvature of the a-SiN:H-coated Si witness wafers.<sup>(12)</sup> The radius of curvature was measured by tracking a microstylus profilometer (Dektak 3030) along the perpendicular axes of each wafer. The resulting total stress values possess an uncertainty of  $\pm 25$  MPa.

**2.4 Aging and Thermal Cycling of Coated PMC's** The PMC's were aged at 371 °C for up to 500 hr. Samples were weighed before heating and again after 25, 50, 100, 200, 300, and 500 hr. Thermal cycling was performed to determine (1) the possible effect of fatigue caused by the plastic deformation of the coating or resin interface and (2) whether the total stress in the coating exceeded the yield stress of the material. All thermal cycling was performed with a Heat Transfer Technologies thermal cycler, model 001. The first protocol involved a 38 °C/min ramp to 232 °C, a 12-min soak at temperature, a 27 °C/min cool-down (liquid-nitrogen assisted) to -18 °C, and a 30-min soak at -18 °C, for a total of 300 cycles. A second protocol used the same temperature cycle except the lower temperature limit was 25 °C rather than -18 °C. One thousand cycles were performed. After 100, 200, 300, 500, and 1000 cycles, the samples were inspected with the electron microscope to look for the onset of cracking.

### 3. RESULTS AND DISCUSSION

In Reference 4, NiCrAlY coatings sputter-deposited on PMR-15 PMC's produced mixed results. The as-deposited coatings demonstrated good adhesion to the PMC's (Fig. 1(a)), but they delaminated when isothermally aged at 399 °C (Fig. 1(b)). These coatings alone will not protect a PMC from oxidation, although they may find application as either a protective overcoat for the oxidation barrier or as an interfacial compliant layer.

**3.1 Plasma-Deposited a-SiN:H Coatings** All the a-SiN:H coatings (0.1 to 10  $\mu\text{m}$ ) displayed good adhesion and conformity to the PMC substrates, irrespective of the PMC fabrication technique (autoclaved or compression molded) (Fig. 2).

The major factors that cause the oxidation performance of uncoated PMC's to vary are (1) the thermal stability of the polymer resin, (2) the carbon fiber, (3) the resin-fiber interface, and (4) the relative resin and fiber volume fraction. Acid digestion studies performed on three separate regions of each sectioned 7.5- by 20-cm PMC coupon were cross-referenced with the C-Scan analysis to establish the uniformity of the resin, fiber, and void content in each coupon. This information ensured that only PMC coupons with similar compositions were coated. All coated samples were aged with equal sized, uncoated controls made from the same fiber and monomer

batch. These precautions minimized variations due to (1) temperature fluctuations during aging, (2) different resin/fiber volume fractions, and (3) differences in batch-to-batch monomer solutions and fiber properties. Isothermal aging of larger (5- by 5-cm) coupons allowed a better measure of the protective value of the coating because the surface area of the deleterious cut-fiber edges constituted proportionally less of the total surface area. The use of smaller (1- by 1-cm) coupons allowed more samples to be simultaneously coated and aged for a statistical comparison.

Because the weight loss of PMC's does not scale linearly with size or surface area, only equal-sized uncoated and coated coupons were compared. Fiber edges impose a profoundly greater influence on the coupon's thermo-oxidative stability than do the resin-rich (top and bottom) surfaces.<sup>(13)</sup> The exposed fibers provide a conduit for rapid oxygen diffusion along the fiber/matrix interface into the bulk of the matrix.

A concern when interpreting weight-loss data is discriminating between the oxidation-induced weight loss and the concurrent weight loss due to anaerobic thermal decomposition of incompletely polymerized oligomers. Although the thermal degradation at 371 °C would not amount to more than 1 percent (total weight loss) for a 24-hr air post-cured sample, this phenomenon can distort the apparent protective value of the coating because the total isothermal weight loss of a coated PMC is <1 percent after 100-hr aging in air.

Analyzing the weight-loss data of coated and control PMC's (Fig. 3) provided the following observations. The a-SiN:H coated, autoclaved PMC's displayed one-third to one-fifth the weight loss of the controls. The weight loss of the coated PMC was dependent on the processing conditions. By contrast, the coatings on the compression-molded PMC's had no effect: the weight-loss data of the coated and uncoated coupons were comparable for the entire aging process. This difference in the coating performance of PMC's that differ only in their method of fabrication is attributed to the effect of the PMC's surface finish on the coating. Although the simulated vacuum bag process produced a rougher surface than did compression molding, the surface was resin-rich and free of the exposed fibers and larger craters prevalent on the compression-molded surfaces. Examples of these phenomena are shown in the electron micrograph of a cross-sectioned, compression-molded composite (Fig. 2(b)). Here, although the high-aspect-ratio craters have been coated, sharp angles and loose fibers create regions of high strains and stresses that undermine the coating when the coated composite is aged.

Monitoring the coated autoclaved composites during thermal aging (after 25, 50, 100, and 200 hr) revealed two events: (1) after 50 to 100 hr, holes formed in the coating on the PMC's edges perpendicular to the fiber axis (see Fig. 4(a)) and (2) very small cracks formed (1- $\mu$ m wide) in some of the coatings, indicative of tensile stress failure. These cracks occurred (predominantly) perpendicular to the fiber direction and almost exclusively in those regions containing fibers on the surface (Fig. 5).

The most important factor affecting the performance of the coating, when isothermally aged, is the existence of cut-fiber ends in the coated coupons. A cross-sectional scanning electron micrograph of the coated PMC cut-fiber edge (Fig. 4(b)) shows a region where the coating has

been deposited on the cut-fiber edge. When aged, the resin between the fiber end and the coating degrades, and disintegrates when metallurgically cross-sectioned, leaving voids beneath the coating (Fig. 4(c)). Also, at the edge of the PMC, the reinforcing effect of the fiber on the resin is expected to be at its weakest, and the localized strain on the coating (due to the  $\alpha$  mismatch) will increase the stress in the coating. The combination produced large cracks in the coating, on only the cut-fiber ends, after 50- to 100-hr aging. By 200 hr, the coating on the edges had begun to flake off. The unprotected edges then permitted accelerated oxidation of the PMC, even though the coating remained strongly adherent to the rest of the PMC (the top, the bottom, and the edges parallel to the fiber direction).

When aged, the coating developed small cracks ( $\sim 1 \mu\text{m}$ ) perpendicular to the fiber direction. These are attributed to the high intrinsic tensile stress augmented by the shrinkage of the coating as hydrogen is evolved. The phenomenon is well known for plasma-deposited a-SiN:H films annealed above the deposition temperature;<sup>(14)</sup> however, we did not expect so much hydrogen to be evolved at this low temperature that it would generate stress-relieving microcracks. Figure 5(b) shows an example of a microcrack in an aged PMC. In this figure, the coating cohesively fails near, but not at, the interface as if it has been pulled apart, demonstrating the excellent adhesion between the coating and the substrate.

The a-SiN:H coatings that were deposited using  $\text{N}_2$  rather than  $\text{NH}_3$  show superior thermal stability. The difference is believed to be due to the intrinsic stress state of the coatings, the total hydrogen concentration, and the hydrogen bonding sites. Nuclear resonance hydrogen profiling of the a-SiN:H coatings (on the Si witness wafers) (deposited using  $\text{NH}_3$ ) showed the initial hydrogen content to be  $\sim 30$  at.%. Annealing the coating at  $900^\circ\text{C}$  for 10 min reduced the hydrogen concentration to  $\sim 4$  at.%. Fourier transform infrared spectroscopy studies indicated that the hydrogen was lost predominantly from nitrogen rather than from silicon bonding sites. These results support the observation that the thermal stability of the coating can be improved by reducing the total quantity of hydrogen incorporated in the coating, by replacing the nitrogen source with a  $\text{N}_2$  rather than  $\text{NH}_3$  precursor.

**3.2 Intrinsic and Thermal Stresses in a-SiN:H Coatings on PMC's** The thermal stress  $\sigma_t$  that develops in the coating results from the elastic strain  $\epsilon_f$  generated at the interface because of different coefficients of thermal expansion  $\alpha$  for the coating f and the matrix s

$$\epsilon_f = (\alpha_f - \alpha_s) (T_{\text{deposition}} - T) \quad (1)$$

$$\sigma_t = (E_f/1 - \nu_f) \epsilon_f \quad (2)$$

Different coating materials experience different magnitudes of thermal stress depending on the relaxation modulus  $E_f/1 - \nu_f$ , Young's modulus E, and Poisson ratio  $\nu$  and will remain intact until the yield/compressive strength of the material is exceeded.

In addition to the thermal stress, the other major factor affecting the performance of the coating is the intrinsic stress  $\sigma_i$ :

$$\sigma_{\text{total}} = \sigma_t + \sigma_i \quad (3)$$

This stress is inherent to the deposition process and the resulting coating morphology. In particular, grain size, grain morphology (equiaxed versus columnar), and the existence of micropores will govern the intrinsic stresses in these coatings. Other factors such as lattice parameter mismatches, point defects, and contaminations are not significant for amorphous coatings.

The intrinsic stress  $\sigma_i$  present in the a-SiN:H coatings was determined by measuring the total stress  $\sigma$  in the coated silicon witness wafer and then subtracting the calculated thermal stress  $\sigma_t$  component;  $\sigma$  was determined from the measured curvature of the coated silicon witness wafer:<sup>(15)</sup>

$$\sigma = [E_s/6(1 - \nu_s)] (t_s^2/t_f R) \quad (4)$$

where  $[E_s/(1 - \nu_s)] = 180$  GPa is the relaxation modulus for the Si(100) wafer,  $t_s = 400$   $\mu\text{m}$  is the thickness of the substrate,  $t_f$  is the coating thickness, and  $R = C^2/8\Delta h$  is the radius of curvature calculated from the bow of the wafer  $\Delta h$  for the measured chord length  $C$ . Stresses averaging 0.11 GPa (tensile), for identical processing conditions, were calculated. The thermal stress component was calculated with Equations (1) and (2) to be  $\sigma_t = -0.047$  GPa (compressive) ( $(E/(1 - \nu)) \sim 100$  GPa,<sup>(16)</sup>  $\alpha_{\text{a-SiN:H}} \sim 1.5 \times 10^{-6}/^\circ\text{C}$ ,<sup>(17)</sup>  $\alpha_{\text{Si(100)}} = 3.2 \times 10^{-6}/^\circ\text{C}$ ,  $T_{\text{measured}} = 25$   $^\circ\text{C}$ , and  $T_{\text{deposited}} = 300$   $^\circ\text{C}$ ). The intrinsic stress component is then,  $\sigma_i^{\text{a-SiN:H}} \sim 0.16$  GPa.

The magnitude of the stresses present in an a-SiN:H coated PMR-II-50/T650-42 PMC over a 400  $^\circ\text{C}$  temperature cycle can be estimated assuming a uniform stress distribution throughout the coating and no plastic deformation of the coating or substrate. Consider initially the  $\alpha$  along each perpendicular axis of the unidirectional PMC. The axial  $\alpha$ ,  $\alpha^{\text{axial}} = 1 \times 10^{-6}/^\circ\text{C}$ ,<sup>(18)</sup> was determined by the carbon fiber  $\alpha$  ( $\alpha_{\text{fiber}}^{\text{axial}} = -0.7 \times 10^{-6}/^\circ\text{C}$ ),<sup>(19)</sup> and the fiber volume fraction. The transverse intraply  $\alpha$ ,  $\alpha^{\text{transverse}} = 30 \times 10^{-6}/^\circ\text{C}$ ,<sup>(18)</sup> is the aggregate of the resin  $\alpha$  ( $\alpha^{\text{resin}} = 50 \times 10^{-6}/^\circ\text{C}$ ), the transverse  $\alpha$  for the fiber ( $\alpha_{\text{fiber}}^{\text{transverse}} = 18 \times 10^{-6}/^\circ\text{C}$ ),<sup>(19)</sup> and the fiber volume fraction. Finally, the interply  $\alpha$  is equivalent to the  $\alpha^{\text{resin}}$  alone. Since the a-SiN:H coatings were deposited at temperatures comparable to the testing temperature of the PMC, all thermal stress developed during the cooldown after the coating was deposited and would change reversibly when the samples were cycled back to the deposition temperature. At 25  $^\circ\text{C}$ ,  $\sigma_t$  components are calculated to be  $\sigma_t^{\text{axial}} = 0.02$  GPa (tensile) and  $\sigma_t^{\text{transverse}} = -1.14$  GPa (compressive) (Eq. (2)), and the total intraplane stress would be  $\sigma^{\text{axial}} \sim 0.18$  GPa and  $\sigma^{\text{transverse}} \sim -0.98$  GPa. At the edges of the PMC, the stress ( $\sigma^{\text{interply}}$ ) would be  $\sim -1.6$  GPa. The ultimate strength and the tensile yield strength for these coatings are unknown, although an estimate of the strength may be obtained from the known values of CVD  $\text{Si}_3\text{N}_4$  films that have a tensile yield strength of 1.0 to 2.5 GPa.<sup>(17)</sup> In



addition, the magnitude of the yield strength is expected to be greater in compression than in tension.

If a deposition temperature significantly lower than the maximum use-temperature were used, a large, tensile thermal stress would develop during the first aging cycle; that is, if  $T_{\text{aging}} - T_{\text{deposition}} = 200 \text{ }^\circ\text{C}$ ,  $\sigma_t^{\text{axial}} \sim -10 \text{ MPa}$ , and  $\sigma_t^{\text{transverse}} \sim 5.7 \text{ GPa}$ . This thermal stress combined with the intrinsic tensile stress would exceed the yield stress of the material. Thus, from stress considerations alone, it is desirable for the coating to be deposited at high temperatures because the compressive thermal stress generated during cooling would be offset by the intrinsic tensile stress component of the coating.

#### 4. CONCLUSIONS

Plasma-deposited silicon nitride offers significant promise as an oxidation barrier coating for PMC's in high-temperature environments. The coating displayed excellent adhesion and conformity to the surface and did not fracture when thermally cycled. The ability of the coating to withstand the sizeable stresses ( $\sim 180 \text{ MPa}$  to  $-1 \text{ GPa}$ ) associated with a large temperature gradient ( $400 \text{ }^\circ\text{C}$ ) and anisotropic thermal expansion coefficients was attributed to its high yield strength and moderate relaxation modulus. When aged at  $371 \text{ }^\circ\text{C}$  in air, the coated PMC's experienced one-third to one-fifth the weight loss of the uncoated PMC for the initial 200 hr. The major factor limiting greater oxidation protection for longer durations was the effect of the cut-fiber ends: the coating on the PMC edges containing these fiber ends spalled after 100-hr aging. The importance of composite fabrication was evidenced by the superior performance of the coatings on simulated vacuum-bagged PMC's in comparison to compression-molded PMC's. This phenomenon was attributed to the surface finish of the compression-molded PMC's.

#### 5. ACKNOWLEDGMENTS

We thank Mathieu Freeman and Dr. Elizabeth Blanquet for the Rutherford backscattering and nuclear resonance hydrogen profiling performed at the SUNY Albany Dynatron Accelerator, Dr. Pilar Herrera-Fierro for the Fourier transform infrared spectroscopy, Frank Terepka for the analytical electron microscopy, and Todd Leonhardt for the metallurgical sample preparation.

#### 6. REFERENCES

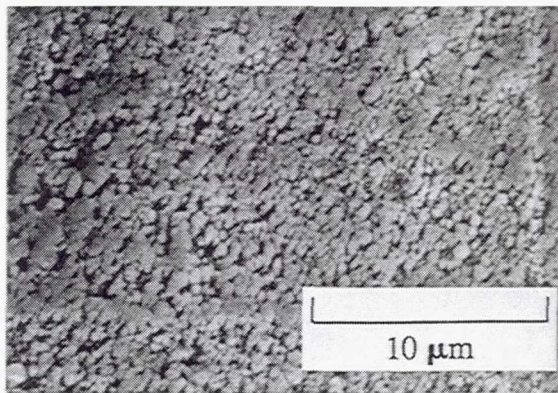
1. M.A. Meador, P.J. Cavano, and D.C. Malarik, Structural Composites: Design and Processing Technologies, Proceedings of the Sixth Annual ASM/ESD Advanced Composite Conference, ASM International, Materials Park, OH, 1990, pp. 529-632.
2. R.D. Vannucci, SAMPE J., 19, (1), 31 (1987).
3. G. Yi and M. Syer, Am. Ceram. Soc. Bull., 70, (7), 1173 (1991).

4. D. Harding, HITEMP Review: Advanced High Temperature Engine Materials Technology Program, 1991, NASA CP-10082, 1991, pp. 10-1 to 10-10.
5. W. Kern and R.S. Rosler, J. Vac. Sci. Technol., 14, (5), 1082 (1977).
6. C.R. Bardnes and C.R. Geesner, J. Electrochem Soc., 107, (2), 98 (1960).
7. K. Niihara and T. Hirai, J. Mater. Sci., 12, 1233 (1977).
8. R.D. Vannucci and D. Cifani, "The 700 °F Properties of Autoclave Cured PMR-2 Composites," NASA TM-100923, 1988.
9. G.M. Porta, et al., Polym. Eng. Sci., 32, (15), 1021 (1992).
10. W.A. Lanford and M.J. Rand, J. Appl. Phys., 49, (4), 2473 (1978).
11. R. Chow, et al., J. Appl. Phys., 53, (8), 5630 (1982).
12. K. Kamata, N. Aizawa, and M. Moriyama, J. Mater. Sci. Lett., 5, 1055 (1986).
13. K.J. Bowles and A. Meyers, "Specimen Geometry Effects on Graphite/PMR-15 Composites During Thermo-Oxidative Aging," NASA TM-87204, 1986.
14. B. Reynes, et al., Thin Solid Films, 203, 87 (1991).
15. G.G. Stoney, Proc. R. Soc., A82, 172 (1909).
16. C. Blaauw, J. Appl. Phys., 54, (9), 5064 (1983).
17. T.F. Retajczyk and A.K. Sinha, Thin Solid Films, 70, 241 (1980).
18. D.A. Elmes and D.C. Gilbert, The Plastics and Rubber Institute 3rd International Conference: Fibre Reinforced Composites, Thermal Stress Analysis in PMR-15 Carbon Fibre Laminates, 35, (1), (1988).
19. Manufacturer's data, "Thornel Product Information," Amoco Performance Products, Inc., Atlanta, GA.

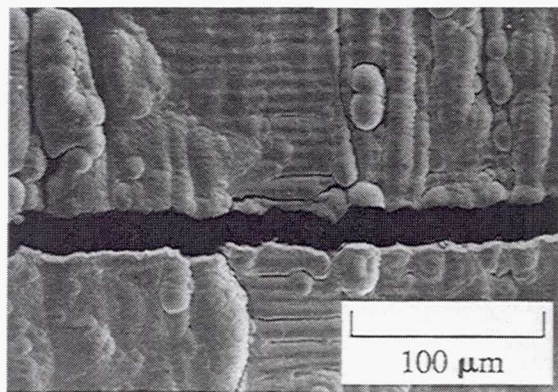
TABLE 1.—COMPOSITION OF a-SiN:H COATINGS DEPOSITED UNDER DIFFERENT CONDITIONS

Experiment <sup>a</sup>	Substrate temperature, °C	Growth rate, Å/min	Silicon/nitrogen		H content
			Wavelength dispersive spectroscopy	Rutherford backscattering	
I	280	280			
II	↓	230	0.66	0.81	31
III		315	.69	.71	31
IIIa		300			
IV		311			
IVa	↓	290			
V		300	.65	.72	27
Va	↓	283			
VI		292		.75	25
VIa		290			

<sup>a</sup>An "a" after a number indicates a duplicated experiment.

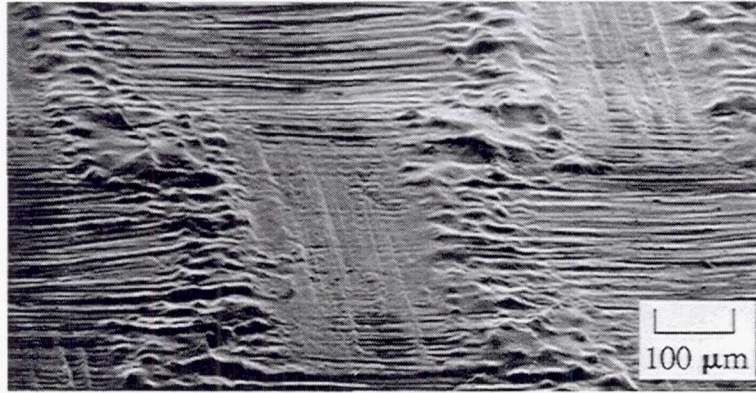


(a) As-deposited.

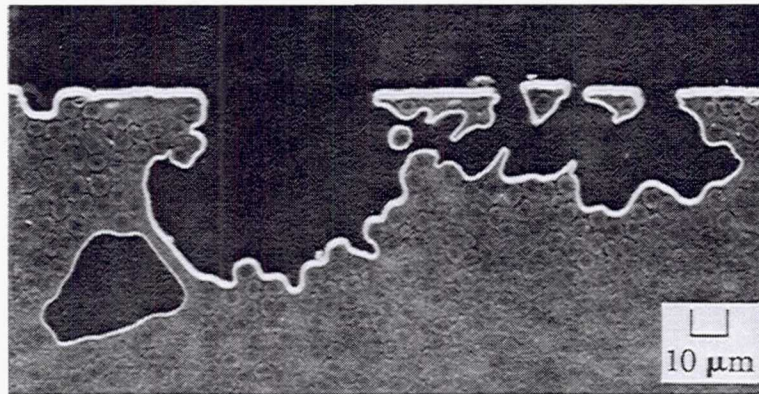


(b) Isothermally aged PMC (164 hrs at 399 °C).

Figure 1.—Electron micrographs of NiCrAlY coatings on PMR-15 substrates.



(a) Autoclaved PMC: top surface at a 75° tilt.



(b) Backscattered image of a cross-sectioned, compression molded PMC; the light area is the coating and the cross-section is perpendicular to the fiber axis.

Figure 2.—Electron micrographs of a-SiN:H coatings on PMR-II-50 PMC's.

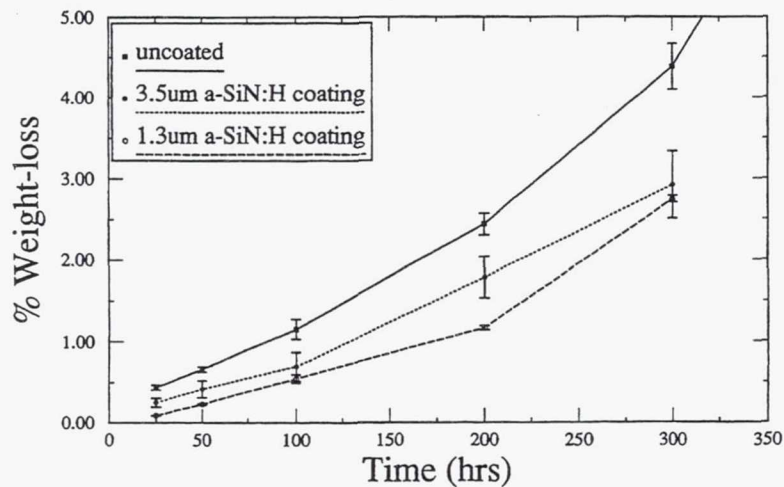
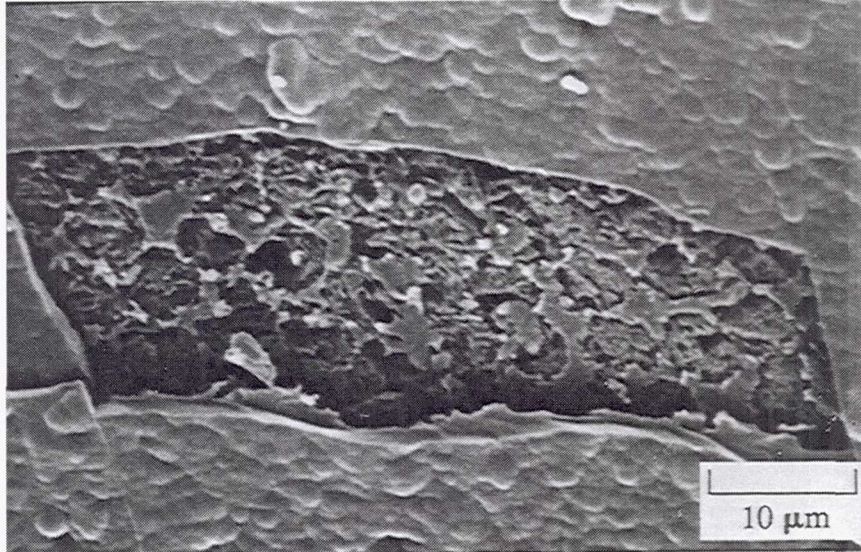
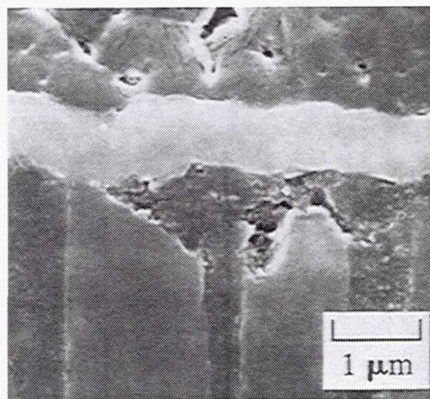


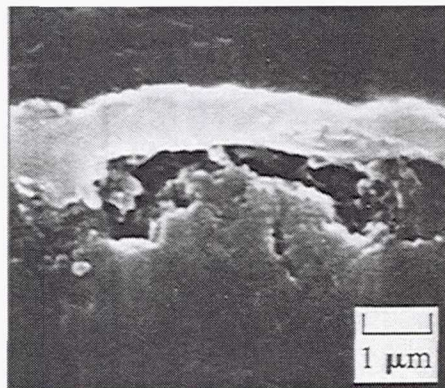
Figure 3.—Isothermal (371 °C) weight-loss data for a-SiN:H coated PMR-II-50 PMC coupons: 1.25 x 1.25 cm coupon size. The coatings were deposited under similar conditions, only the thickness varied. The error bars are 95% confidence intervals.



(a) Aged 100 hrs at 371 °C. Region of delamination at the cut-fiber edge; fiber perpendicular to the coated surface.

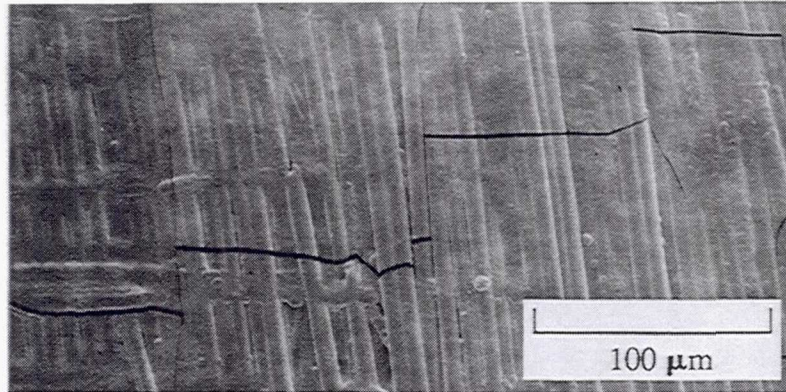


(b) Metallurgically cross-sectioned, fiber direction is in the plane of the micrograph perpendicular to the coating.

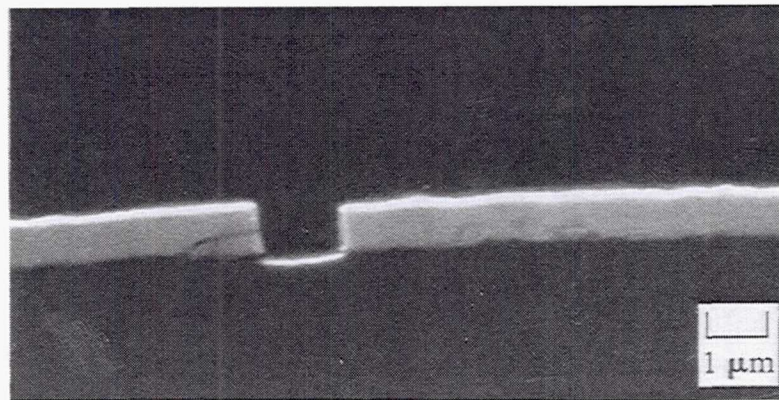


(c) Same as b, except, coupon was thermally cycled, 25 to 232 °C for 200 cycles, then aged for 25 hrs at 371 °C.

Figure 4.—Electron micrographs of the cut-fiber edge of an a-SiN:H coated PMC.



(a) Top surface at  $75^\circ$  tilt; fiber direction is top-to-bottom and perpendicular to the fracture.



(b) Backscattered image of a cross-sectioned, coated, coupon showing the microcrack. Fiber direction is left-to-right in the plane of the micrograph. Fracture occurred within the coating near, but not at, the interface.

Figure 5.—Electron micrographs of the tensile stress induced microcracks in the a-SiN:H coating.

# REPORT DOCUMENTATION PAGE

Form Approved  
OMB No. 0704-0188

Public reporting burden for this collection of information is estimated to average 1 hour per response, including the time for reviewing instructions, searching existing data sources, gathering and maintaining the data needed, and completing and reviewing the collection of information. Send comments regarding this burden estimate or any other aspect of this collection of information, including suggestions for reducing this burden, to Washington Headquarters Services, Directorate for Information Operations and Reports, 1215 Jefferson Davis Highway, Suite 1204, Arlington, VA 22202-4302, and to the Office of Management and Budget, Paperwork Reduction Project (0704-0188), Washington, DC 20503.

<b>1. AGENCY USE ONLY (Leave blank)</b>	<b>2. REPORT DATE</b> July 1993	<b>3. REPORT TYPE AND DATES COVERED</b> Technical Memorandum	
<b>4. TITLE AND SUBTITLE</b> Protective Coatings for High-Temperature Polymer Matrix Composites		<b>5. FUNDING NUMBERS</b>  WU-510-01-50	
<b>6. AUTHOR(S)</b>  David R. Harding, James K. Sutter, and Demetrios Papadopoulos			
<b>7. PERFORMING ORGANIZATION NAME(S) AND ADDRESS(ES)</b>  National Aeronautics and Space Administration Lewis Research Center Cleveland, Ohio 44135-3191		<b>8. PERFORMING ORGANIZATION REPORT NUMBER</b>  E-8013	
<b>9. SPONSORING/MONITORING AGENCY NAME(S) AND ADDRESS(ES)</b>  National Aeronautics and Space Administration Washington, D.C. 20546-0001		<b>10. SPONSORING/MONITORING AGENCY REPORT NUMBER</b>  NASA TM-106276	
<b>11. SUPPLEMENTARY NOTES</b> Prepared for the 25th International SAMPE Technical Conference sponsored by the Society for the Advancement of Material and Process Engineering, Philadelphia, Pennsylvania, October 26-28, 1993. David R. Harding, Sverdrup Technology, Inc., Lewis Research Center Group, 2001 Aerospace Parkway, Brook Park, Ohio 44142; James K. Sutter, NASA Lewis Research Center; and Demetrios Papadopoulos, Case Western Reserve University, Cleveland, Ohio 44106 and NASA Resident Research Associate at Lewis Research Center. Responsible person, James K. Sutter, (216) 433-3226.			
<b>12a. DISTRIBUTION/AVAILABILITY STATEMENT</b>  Unclassified - Unlimited Subject Category 24		<b>12b. DISTRIBUTION CODE</b>	
<b>13. ABSTRACT (Maximum 200 words)</b>  Plasma-enhanced chemical vapor deposition was used to deposit silicon nitride on graphite-fiber-reinforced polyimide composites to protect against oxidation at elevated temperatures. The adhesion and integrity of the coating were evaluated by isothermal aging (371 °C for 500 hr) and thermal cycling. The amorphous silicon nitride (a-SiN:H) coating could withstand stresses ranging from approximately 0.18 GPa (tensile) to -1.6 GPa (compressive) and provided a 30 to 80 percent reduction in oxidation-induced weight loss. The major factor influencing the effectiveness of a-SiN:H as a barrier coating against oxidation is the surface finish of the polymer composite.			
<b>14. SUBJECT TERMS</b>  Coating; Polymer matrix composite; Oxidation reduction; Stresses		<b>15. NUMBER OF PAGES</b> 16	
		<b>16. PRICE CODE</b> A03	
<b>17. SECURITY CLASSIFICATION OF REPORT</b> Unclassified	<b>18. SECURITY CLASSIFICATION OF THIS PAGE</b> Unclassified	<b>19. SECURITY CLASSIFICATION OF ABSTRACT</b> Unclassified	<b>20. LIMITATION OF ABSTRACT</b>